ATMOSPHERIC SCIENCE LETTERS
Atmos. Sci. Let. **15**: 13–20 (2014)
Published online 31 July 2013 in Wiley Online Library
(wileyonlinelibrary.com) **DOI:** 10.1002/asl2.456

RMetS
Royal Meteorological Society

Surface air temperature variability in global climate models

Richard Davy* and Igor Esau

Nansen Environmental and Remote Sensing Centre, Centre for Climate Dynamics (SKD), 5006, Bergen, Norway

**Correspondence to:*
Richard Davy, Nansen Environmental and Remote Sensing Centre, Centre for Climate Dynamics (SKD), Thormøhlensgt. 47, 5006 Bergen, Norway.
E-mail: *richard.davy@nersc.no*

Received: 22 April 2013
Revised: 10 July 2013
Accepted: 10 July 2013

Abstract

New results from the Coupled Model Intercomparison Project phase 5 (CMIP5) and multiple global reanalysis datasets are used to investigate the relationship between the mean and standard deviation (SD) in the surface air temperature (SAT) at intra- and inter-annual timescales. A combination of a land–sea mask and orographic filter was used to investigate the geographic region with the strongest correlation and in all cases this was found to be for low-lying over-land locations. This result is consistent with the expectation that differences in the effective heat capacity of the atmosphere are an important factor in determining the SAT response to forcing.

Keywords: **climate; climate change; planetary boundary layer; temperature; CMIP5**

1. Introduction

The surface air temperature (SAT) and its various properties (diurnal and seasonal range and extremes, trends and variability) are some of the most widely used metrics of global climate and climate change (IPCC AR4, 2007). This is to be expected given that the SAT is such a readily measurable, and anthropically important, variable. The variability of the SAT at a given timescale is determined by three factors: the magnitude of the forcing, any feedback processes and the effective heat capacity of the system (Hasselmann, 1976; Frankignoul and Hasselmann, 1977; Hansen *et al.*, 2011). Through consideration of the near-surface energy balance it has been demonstrated that there is an inverse dependency of the magnitude of changes in SAT on the effective heat capacity of the atmosphere (Esau *et al.*, 2012, hereafter EDO12) and soil (Seneviratne *et al.*, 2010). The effective heat capacity of the atmosphere has been shown to be directly proportional to the depth of the planetary boundary layer (PBL) (Esau and Zilitinkevich, 2010) whereas the soil heat capacity depends on the soil moisture available (deVries, 1963). In both cases an increased heat capacity acts to dampen near-surface temperature trends. It may be expected that an increase in forcing will affect the PBL depth as well as temperature. For example, on the diurnal timescale much of the heating in the morning transition goes into increasing the PBL depth from the relatively shallow nocturnal boundary layer to a much deeper convective boundary layer. However, in our analysis such changes are already accounted for in the base-line climatology; and it has been shown that increases in the boundary-layer depth due to enhanced forcing is a relatively small effect on climatological timescales (Figure S1, Supporting Information).

This mechanism – PBL response – suggests that some relations between metrics of the SAT are innate to the thermodynamics of the climate system. For example, the strong positive correlation between SAT trends and variability that exists across the globe, as has been shown in observations, reanalysis and CMIP3 datasets (EDO12). This may be expected given that SAT trends and variability are both manifestations of the magnitude of SAT response to forcing. EDO12 noted that such features of the PBL response, e.g. the linear relationship between mean and standard deviation (SD) of SAT, were not to be found in high-altitude locations, such as Greenland. At such locations the surface air is exposed to the free atmosphere, and as such one would not expect to see the same PBL response. Here, we make use of this characteristic of PBL-response theory to provide a test of this theory in comparison with alternate explanations of this relationship between SAT mean and SD.

The strongest signal of PBL response is expected to be seen in locations with shallow boundary layers, and thus a low effective heat capacity. The shallowest boundary layers are found over land in locations with consistent negative surface sensible heat flux, which leads to a strong stable thermal stratification. Therefore, we expect to see the strongest signal of PBL response at over-land locations. As this mechanism is driven by the turbulent mixing that characterizes the PBL, we expect there to be a weaker signal in high-altitude locations where the PBL is exposed to the free atmosphere. This prediction opens the possibility to distinguish the effects of the PBL response from the response of soil moisture (Quesada *et al.*, 2012) as they are not expected to change with altitude. There has been some discussion of the vertical dependency of the temperature variability and

the causes for this; for example Wang *et al.* (2005) demonstrated that the North Atlantic Oscillation signal was a largely tropospheric phenomenon, whereas the Arctic Oscillation signal could penetrate into the stratosphere. This relates to discussions on the vertical profile of recent global warming and as to what role local processes play in determining the profile of atmospheric warming. There has been some indication from the work of Weber *et al.* (1994) that one such pattern predicted from PBL-response theory – the asymmetric response of diurnal minimum and maximum temperatures – is constrained to the PBL, but the reason for this asymmetry was not identified in their work. We further investigate the cause for such asymmetries in temperature trends by extending the analysis of SAT response in mountainous and low-lying locations from station data, as in Weber *et al.* (1994), to a global analysis using reanalyses and climate models. Such asymmetries may appear in observations, but not in global climate models (GCMs) where the vertical exchange is not explicitly resolved and is instead represented through parameterization schemes. Such schemes have fundamental problems in representing turbulence as they are based on eddy diffusivity schemes (K-schemes) which means the turbulence is modelled as a diffusion operator, not as an advection operator. The prediction that these relationships should be weaker over oceans and in locations exposed to the free atmosphere allows us to falsify the PBL-response mechanism by comparing the strength of such relationships with and without the use of land and orographic filters.

One of the biggest challenges in assessing the role of the PBL in Earth's climate system is the limitations on assessing the climatology of the PBL (Seidel *et al.*, 2010). Seidel *et al.* (2012) compared the climatology of the PBL over the continental United States and Europe between climate models, reanalysis and radiosonde observations. They found diurnal, seasonal and geographical structures of the PBL climatology in models and observations. However, there were significant biases in the model PBL depth for shallow PBLs as the models have trouble simulating conditions of stable stratification and over estimate the PBL depth. Thus, the diurnal and seasonal cycles are only reproduced by models because the PBL is so much deeper during the day than at night and during the summer than in winter. There are still large uncertainties in the depth and variability of shallow PBLs in models, and they have trouble capturing the morning and evening transition periods (Denning *et al.*, 2008). PBL depth data were available in the ERA-Interim reanalysis, and we have used this for verification of the proposed relationship between the depth of the mixed layer and SAT trends and variability. However, it should be noted that the PBL data are generally not available for GCM results, therefore it is necessary to use a proxy for the PBL mixing, such as the mean SAT (EDO12). It has been established that PBL response predicts an inverse relationship between the mean and SD of SAT (EDO12). We have used a simple least squares linear regression analysis to investigate this relationship on intra- and inter-annual timescales, using data from Coupled Model Intercomparison Project phase 5 (CMIP5) results and various reanalysis datasets.

2. Data sets

The data used for this study were taken from the CMIP5 results and various global reanalysis projects, the data for which is hosted by the National Center for Atmospheric Research (NCAR). The temperature data were taken from the last 30 years of the 'historical' runs of the CMIP5, and from the same years in the reanalysis datasets with the exception of the Japanese 25-year reanalysis project (JRA25).

The historical simulations of the CMIP5 are run using changing conditions consistent with observations including: atmospheric composition, including anthropogenic and volcanic influences; solar forcing; land use changes and emissions or concentrations of short-lived species and natural and anthropogenic aerosols (Taylor *et al.*, 2009). These simulations are performed by coupled ocean–atmosphere GCMs. We have used results from eight of the groups that contributed to CMIP5, which offered a reasonable cross-section of GCM results: CSIRO Australia's CSIRO Mk3.5 (Gordon *et al.*, 2010); the Japan agency for Marine-Earth Science and Technology and National Institute for Environmental Studies MIROC-ESM-CHEM (Watanabe *et al.*, 2011) and MIROC5 (Watanabe *et al.*, 2010); the French National Centre for Meteorological Research's CNRM-CM5 (Voldoire *et al.*, 2010); the UK Met Office Hadley Centre's HadCM3 and HadGEM2-AO (Collins *et al.*, 2011); the Institute for Numerical Mathematics' INMCM4 (Volodin, *et al.*, 2010) and the Norwegian Climate Centre's NorESM (Iversen *et al.*, 2012).

The reanalysis datasets used were: the JRA25 (Onogi *et al.*, 2007); the National Centers for Environmental Prediction (NCEP) Climate Forecast System Reanalysis (CFSR) (Saha *et al.*, 2010); the European Center for Medium-range Weather Forecast (ECMWF) Interim reanalysis (ERA-Interim) (Dee *et al.*, 2011); the National Oceanic and Atmospheric Administration (NOAA) 20th Century Reanalysis v2 (Compo *et al.*, 2011) and the NCEP/NCAR reanalysis I (Kalnay *et al.*, 1996).

3. Methods

Each of the GCMs and reanalysis has associated orographic data and a land/sea mask. An orographic filter, 'Orog', was created that removed all data corresponding to locations where the surface elevation is greater than 1 km. This height threshold was chosen as a characteristic height for mountainous terrain, and the results are insensitive to a 20% variation in

this threshold. Locations with surface elevation greater than 1 km ('highland') are assumed to be exposed to the free atmosphere. It should be noted that this filtering technique will also remove high-altitude, but relatively flat, areas which would not be expected to have the same exposure to the free atmosphere. However, since there was not a ready method to differentiate between mountainous and high-altitude, plain locations, we chose to use a simplified filtering technique which would ensure the removal of mountainous locations. The land–sea mask of each dataset was used as a 'land' filter, to select only those grid points which lay over land. The combination of the orographic and land filters was used to select only low-lying, over-land ('lowland') locations, where we anticipate the strongest signal of the PBL response.

Monthly means of the diurnal-mean SAT were obtained for each dataset, covering the last 30 years of the CMIP5 'historical' simulations (1976–2005). For each dataset, a time series of temperature anomalies was calculated by removing the 30-year monthly means from the monthly temperature time series. So for each month the climatological mean was removed to obtain the anomaly:

$$T'_{\text{month}} = T_{\text{month}} - \frac{1}{n}\sum_{n\ \text{years}} T_{\text{month}}$$

The temperature statistics (SD) were calculated from the monthly anomalies after the removal of a fourth order polynomial trend from the time series (Braganza *et al.*, 2003).

The inter-annual correlations were calculated by taking the climatological (30 years) mean and the SD of the SAT at each location, and correlating these across all locations, using an area-weighted correlation. This is given by:

$$C^{\text{SD}}_{\text{mean}} = \frac{\text{cov}\,(T_{\text{mean}}, \sigma_T; A)}{\sqrt{\text{cov}\,(T_{\text{mean}}, T_{\text{mean}}; A)\,\text{cov}\,(\sigma_T, \sigma_T; A)}}$$

where T_{mean} is the climatological mean temperature (K), σ_T is the SD (K), A is the surface area of each grid box (m^2) and $\text{cov}(x, y; w)$ is the covariance of x and y with weighting function, w, and is given by:

$$\text{cov}(x, y; w) = \frac{\sum_i w_i \left(x_i - \frac{\sum_j x_j w_j}{\sum_j w_j}\right)\left(y_i - \frac{\sum_j y_j w_j}{\sum_j w_j}\right)}{\sum_j w_j}$$

The intra-annual correlations were calculated at each location by correlating the mean and SD of each month. These correlations were filtered for significance ($p < 0.05$) prior to using an area-weighted mean to obtain a single, global-mean correlation.

For the ERA-Interim reanalysis dataset, the climatological mean (average over indicated years) of the reciprocal of the 3-hourly boundary-layer depth was calculated. This averaging of the reciprocal boundary-layer depth reflects the observation that the temperature response to a given forcing is reciprocally dependant on the boundary-layer depth on all timescales. This averaging puts a strong emphasis on locations and periods with shallow boundary layers which are generally poorly defined by model parameterization schemes. The PBL depth in the ERA-Interim reanalysis is defined from a threshold Flux-Richardson number, integrated between model levels. Analysis of different methods for determining the PBL depth have shown that definitions based on the Richardson number are the most reliable (Seibert *et al.*, 2000; Zilitinkevich *et al.*, 2007). The Global Energy and Water EXchanges project's (GEWEX) Atmospheric Boundary Layer Study (GABLS) projects showed that model schemes give an uncertainty in the PBL depth between 50 and 100% throughout the diurnal cycle (Svensson *et al.*, 2011) and that for a given uncertainty in the PBL depth, averaging over reciprocal boundary-layer depth gives a lower absolute uncertainty in the mean PBL depth.

4. Results

It is the shallower boundary layers, found over land and at high latitudes (Figure 1(a)), where we expect to see the strongest temperature response. We also see a strong seasonal variation in the depth of the PBL, with the shallower boundary layers found over land during the winter months (Figure 1(b)). Note that the averaging of the reciprocal of boundary-layer depth gives heavy weight to the periods with shallow boundary layers. As such, the characteristic boundary-layer depth over land is much shallower (100 m) than that found over ocean (1 km), as it is only over land where you find the very shallow boundary layers associated with strongly stably stratified conditions. In the winter boundary layers over land can be of the order 10 m, and it is these very shallow boundary layers which dominate the climatological mean of reciprocal boundary-layer depth. For the ERA-Interim reanalysis, we find a strong correlation between the reciprocal of the PBL depth and both the SAT trends ($r = 0.84$, $p < 0.05$) and SD ($r = 0.97$, $p < 0.05$) intra-annually (Figure 1(a)). We also find strong relationships inter-annually by comparing the climatology of the reciprocal PBL depth and SAT variability at different locations around the globe (Figure 1(b)).

Figure 2(a) shows the correlation of the mean and inter-annual SD of the SAT from various GCMs. A negative correlation means that the locations with the colder climatological mean temperature have greater variability than the warmer locations. Application of the orographic filter always improves the correlation and the strongest correlations are found for lowland locations, with the exception of the results from NorESM where the over-land correlation is especially

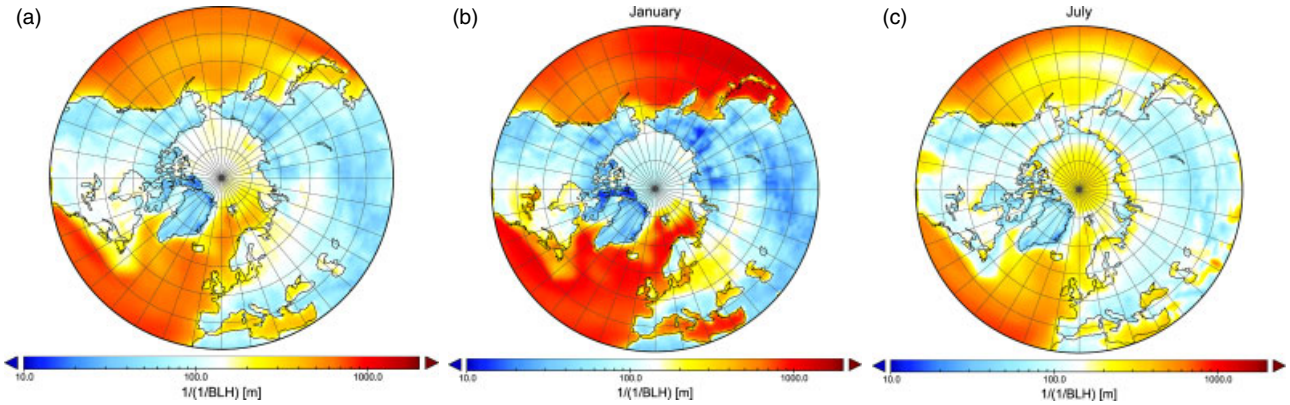

Figure 1. The reciprocal of the climatological mean of the reciprocal boundary-layer depth for (a) annual and (b) January and July data for the Northern Hemisphere, from ERA-Interim.

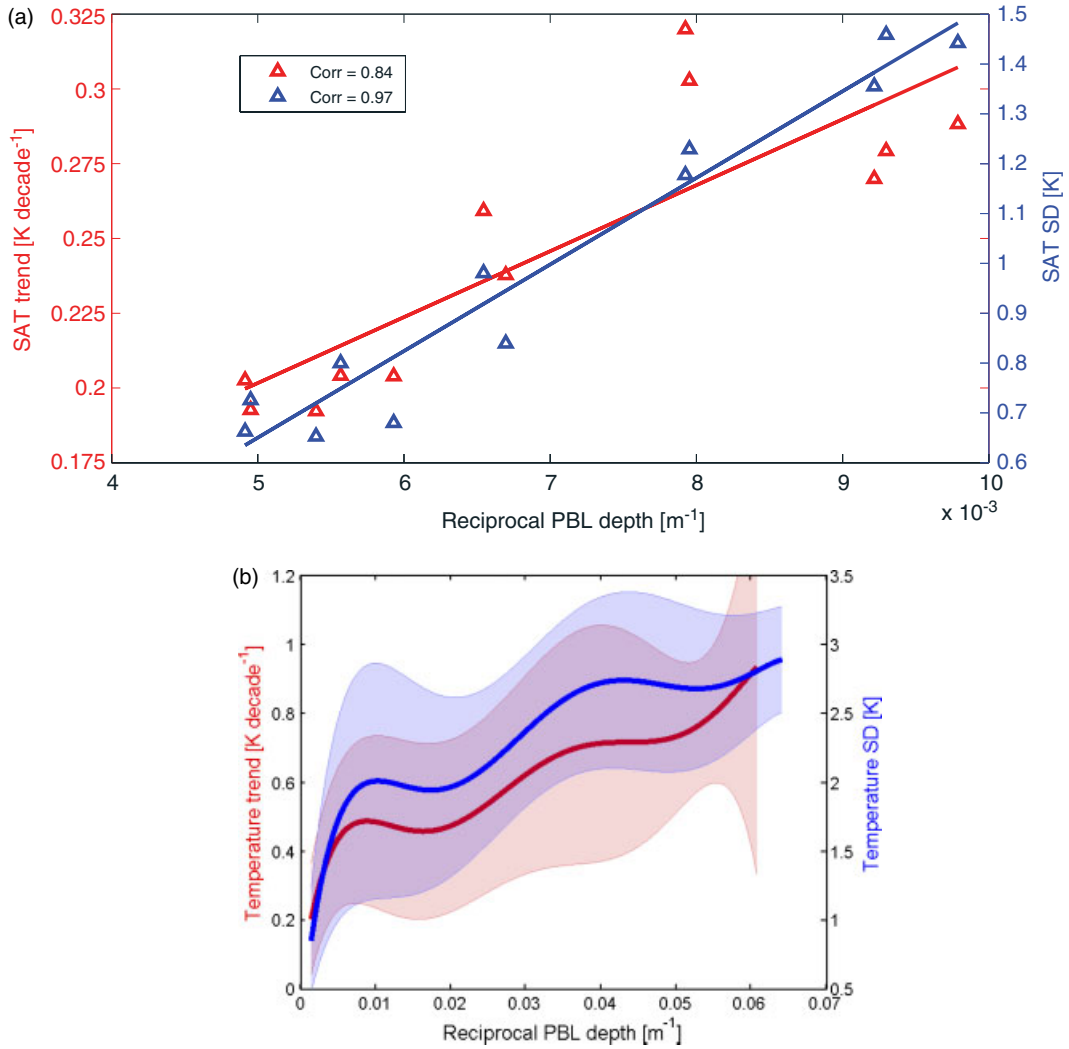

Figure 2. (a) The area-weighted SD and linear trend in SAT as a function of the monthly mean of the reciprocal boundary-layer depth for the Northern Hemisphere, from ERA-Interim reanalysis. (b) The inter-annual standard deviation and trend in SAT as a function of the mean of the reciprocal boundary-layer depth from ERA-Interim. The thick line represents the mean of the binned value, and the shaded area is one standard deviation within each bin. Inter-annually there is an overall correlation of $r = 0.56$, $p < 0.05$ between the reciprocal PBL depth and SAT trends, and a correlation of $r = 0.60$, $p < 0.05$ between reciprocal PBL depth and SD in SAT.

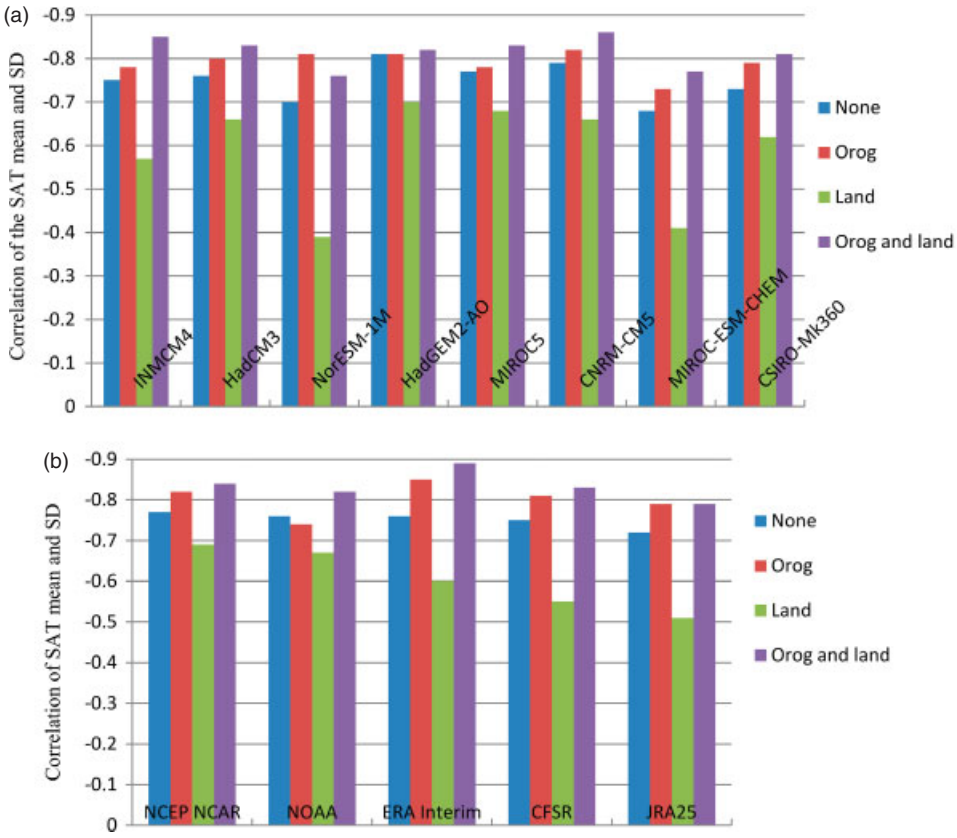

Figure 3. The inter-annual correlation of the mean and SD in SAT from (a) CMIP5 models and (b) reanalysis calculated after applying a land–sea mask (Land) and an orographic filter (Orog).

poor. We find the same result in the reanalysis datasets where the strongest correlations are always found for lowland locations (Figure 2(b)).

In all cases, the biggest difference in the correlation comes with the addition of the orographic filter to the land-filtered data. The significance of these differences in the correlations can be seen from the difference in the number of data points used in each case. The highland regions represent 13% of the total number of grid points so the addition of the orographic filter to the global data does not significantly improve the correlation. However, the highland locations represent 41% of the over-land grid points; hence the largest improvement in the correlations is seen in the application of the orographic filter to the over-land data. This is also why we see a drop in the correlation after the application of the land filter to the global data: the fraction of grid points which correspond to highland locations is increased.

We find a similar pattern in the area-weighted average intra-annual correlations (Figure 3). A positive correlation indicates that the warmer months have the greater variability and a negative correlation indicates that the colder months have the higher variability – the result anticipated from PBL-response theory. Therefore in the regions where the PBL response plays a more dominant role in determining SAT variability we would expect a stronger negative correlation. Such strong negative correlations are found for overland locations and, with the exception of the INMCM4 and NOAA 20th Century Reanalysis results, the strongest correlations are found for lowland locations. This pattern of intra-annual correlations can be readily understood from the associated geographical distribution.

There is a very similar geographical pattern to the intra-annual correlations in all CMIP5 models and reanalysis with strong negative correlations across the middle- and high-latitude continental regions and over the Arctic Ocean (Figure 4). There are two bands of strong positive correlation over the Atlantic and Pacific oceans. Hence the biggest difference in the geographical mean correlations (Figure 3) comes from the application of the land filter. These bands of positive correlation – suggesting the warmer months are more variable than colder months – lie over the storm tracks and reflect the high inter-annual variations in the summer air temperatures over these regions. This is to be expected as SATs over open ocean are governed by the sea-surface temperature (SST). In winter there is a relatively deep ocean mixed layer and relatively small inter-annual variations in the radiative forcing, and so the SST is relatively consistent from year to year. However, in the summer time the water is warmer, the mixed layer is shallower (and so the effective heat capacity is lower), and so the strong variations in the radiative forcing from inter-annual changes in the cloud cover can strongly affect the SST, and thus the SAT (Figure 5).

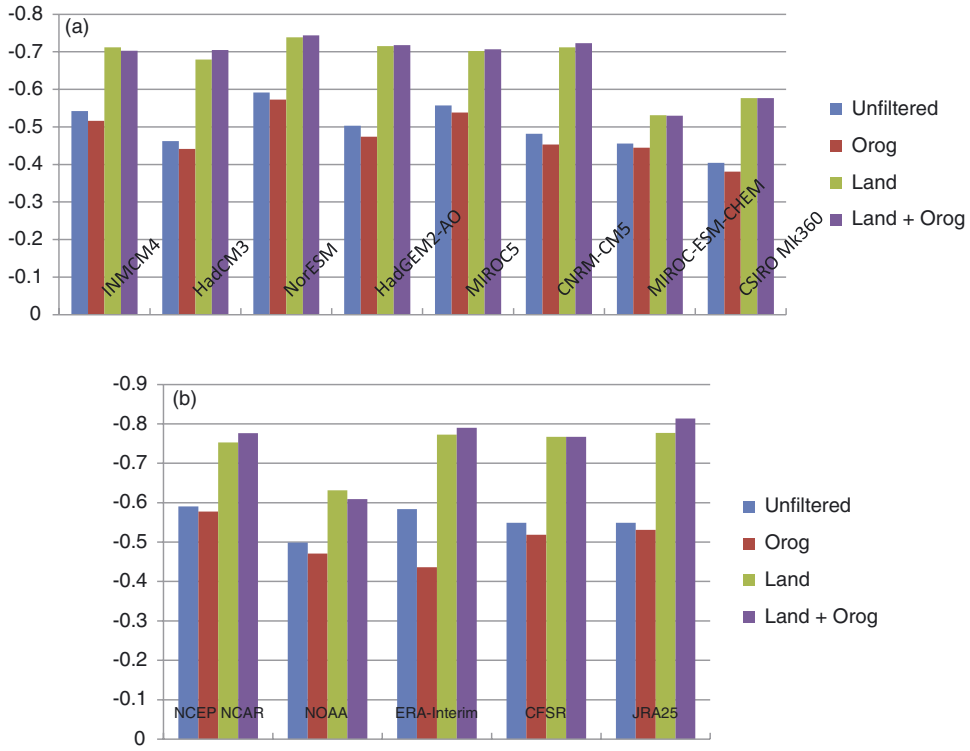

Figure 4. The Northern Hemisphere area-weighted mean of intra-annual correlations of the mean and SD in SAT from (a) CMIP5 models and (b) reanalysis calculated after applying a land–sea mask (Land) and an orographic filter (Orog).

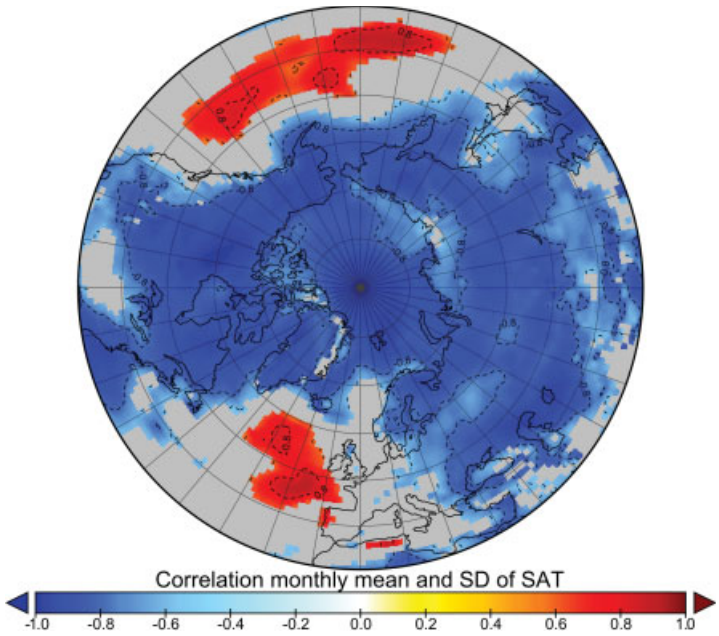

Figure 5. The monthly intra-annual correlation of mean and SD of SAT from ERA-Interim.

5. Conclusions

In this study, we used the results from the latest phase of the CMIP to identify one of the climatological features of SAT variability: the strong negative correlation between SAT mean and variability. This result was confirmed in multiple reanalysis datasets on inter-annual and intra-annual timescales. This relation is consistent with the PBL-response hypothesis that the differences in the SAT variability are, in part, due to variations in the effective heat capacity of the atmosphere such that, the lower the effective heat capacity, the greater the SAT response to a given forcing (EDO12). This was confirmed using the PBL depth data available in the ERA-Interim reanalysis dataset, where we found a strong link between the climatology of the PBL and the SAT response to forcing on intra- and inter-annual timescales. Indeed, these results

are difficult to explain on the basis of soil moisture and cloud cover changes alone. When we include the highland locations where the PBL is exposed to the free atmosphere – and as such is not expected to produce the same response – we find a weaker correlation between the SAT mean and SD. This is in agreement with our expectation that this relationship is a consequence of the PBL response.

Supporting information

The following supporting information is available:

Figure S1. The trend in boundary-layer depth in percentage per decade from ERA-Interim over the period 1979–2010.

Acknowledgements

This work has been funded by the Norwegian Research Council FRINAT project *PBL-feedback* 191516/V30.

References

Braganza K, Karoly DJ, Hirst AC, Mann ME, Stott P, Stouffer RJ, Tett SFB. 2003. Simple indices of global climate variability and change: Part I, variability and correlation structure. *Climate Dynamics* **20**: 491–502.

Collins WJ, Bellouin N, Doutriaux-Boucher M, Gedney N, Halloran P, Hinton T, Hughes J, Jones CD, Joshi M, Liddicoat S, Martin G, O'Connor F, Rae J, Senior C, Sitch S, Totterdell I, Wiltshire A, Woodward S. 2011. Development and evaluation of an Earth-system model – HadGEM2. *Geoscientific Model Development* **4**: 1051–1075, DOI: 10.5194/gmd-4-1051-2011.

Compo GP, Whitaker JS, Sardeshmukh PD, Matsui N, Allan RJ, Yin X, Gleason BE, Vose RS, Rutledge G, Bessemoulin P, Bronnimann S, Brunet M, Crouthamel RI, Grant AN, Groisman PY, Jones PD, Kruk MC, Kruger AC, Marshall GJ, Maugeri M, Mok HY, Nordli Ø, Ross TF, Trigo RM, Wang XL, Woodruff SD, Worley SJ. 2011. The twentieth century reanalysis project. *Quarterly Journal of the Royal Meteorological Society* **137**: 1–28, DOI: 10.1002/qj.766.

Dee DP, Uppala SM, Simmons AJ, Berrisford P, Poli P, Kobayashi S, Andrae U, Balmaseda MA, Balsamo G, Bauer P, Bechtold P, Beljaars ACM, van de Berg L, Bidlot J, Bormann N, Delsol C, Dragani R, Fuentes M, Geer AJ, Haimberger L, Healy SB, Hersbach H, Holm EV, Isaksen L, Kållberg P, Kohler M, Matricardi M, McNally AP, Monge-Sanz BM, Morcrette J-J, Park B-K, Peubey C, de Rosnay P, Tavolato C, Thepaut J-N, Vitart F. 2011. The ERA-Interim reanalysis: configuration and performance of the data assimilation system. *Quarterly Journal of the Royal Meteorological Society* **137**: 553–597, DOI: 10.1002/qj.828.

Denning AS, Zhang N, Yi C, Branson M, Davis K, Kleist J, Bakwin P. 2008. Evaluation of modelled atmospheric boundary layer depth at the WLEF tower. *Agricultural and Forest Meteorology* **148**: 206–215.

DeVries DA. 1963. Thermal properties of soils. In *Physics of Plant Environment*, van Wijk WR (ed). North-Holland Publishing Company: Amsterdam.

Esau I, Zilitinkevich S. 2010. On the role of the planetary boundary layer depth in the climate system. *Advances in Science and Research* **4**: 63–69, DOI: 10.5194/asr-4-63-2010.

Esau I, Davy R, Outten S. 2012. Complementary explanation of temperature response in the lower atmosphere. *Environmental Research Letters* **7**: 044026, DOI: 10.1088/1748-9326/7/4/044026.

Frankignoul C, Hasselmann K. 1977. Stochastic climate models, part II application to sea-surface temperature anomalies and thermocline variability. *Tellus* **29**: 4.

Gordon HB, O'Farrell S, Collier M, Dix M, Rotstayn L, Kowalczyk E, Hirst T, Watterson I. 2010. The CSIRO Mk3.5 Climate Model, technical report No. 21. The Centre for Australian Weather and Climate Research, Aspendale, Victoria, Australia.

Hansen J, Sato M, Kharecha P, von Schuckmann K. 2011. Earth's energy imbalance and implications. *Atmospheric Chemistry and Physics* **11**: 13421–13449, DOI: 10.5194/acp-11-13421-2011.

Hasselmann K. 1976. Stochastic climate models. *Tellus* **28**: 6.

Iversen T, Bentsen M, Bethke I, Debernard JB, Kirkevåg A, Seland Ø, Drange H, Kristjansson JE, Medhaug I, Sand M, Seierstad IA. 2012. The Norwegian Earth System Model, NorESM1-M – Part 2: climate response and scenario projections. *Geoscientific Model Development Discussions* **5**: 2933–2998.

Kalnay E, Kanamitsu M, Kistler R, Collins W, Deaven D, Gandin L, Iredell M, Saha S, White G, Woollen J, Zhu Y, Chelliah M, Ebisuzaki W, Higgins W, Janowiak J, Mo KC, Ropelewski C, Wang J, Leetmaa A, Reynolds R, Jenne R, Joseph D. 1996. The NCEP/NCAR 40-year reanalysis project. *Bulletin of the American Meteorological Society* **77**: 437–470.

Onogi K, Tsutsui J, Koide H, Sakamoto M, Kobayashi S, Hatsushika H, Matsumoto T, Yamazaki N, Kamahori H, Takahashi K, Kadokura S, Wada K, Kato K, Oyama R, Ose T, Mannoji N, Taira R. 2007. The JRA-25 reanalysis. *Journal of the Meteorological Society of Japan* **85**(3): 369–432.

Quesada B, Vautard R, Yiou P, Hirschi M, Seneviratne SI. 2012. Asymmetric European summer heat predictability from wet and dry southern winters and springs. *Nature Climate Change* **2**: 736–741, DOI: 10.1038/nclimate1536.

Saha S, Moorthi S, Pan H-L, Wu X, Wang J, Nadiga S, Tripp P, Kistler R, Woollen J, Behringer D, Liu H, Stokes D, Grumbine R, Gayno G, Wang J, Hou Y-T, Chuang H-Y, Juang H-MH, Sela J, Iredell M, Treadon R, Kleist D, Van Delst P, Keyser D, Derber J, Ek M, Meng J, Wei H, Yang R, Lord S, Van Den Dool H, Kumar A, Wang W, Long C, Chelliah M, Xue Y, Huang B, Schemm J-K, Ebisuzaki W, Lin R, Xie P, Chen M, Zhou S, Higgins W, Zou C-Z, Liu Q, Chen Y, Han Y, Cucurull L, Reynolds RW, Rutledge G, Goldberg M. 2010. The NCEP climate forecast system reanalysis. *Bulletin of the American Meteorological Society* **91**: 1015–1057, DOI: 10.1175/2010BAMS3001.1.

Seibert P, Beyrich F, Gryning S-E, Joffre S, Rasmussen A, Tercier P. 2000. Review and intercomparison of operational methods for the determination of the mixing height. *Atmospheric Environment* **34**(7): 1001–1027.

Seidel DJ, Ao CO, Li K. 2010. Estimating climatological planetary boundary layer heights from radiosonde observations: comparison of methods and uncertainty analysis. *Journal of Geophysical Research* **115**: D16113, DOI: 10.1029/2009JD013680.

Seidel DJ, Zhang Y, Beljaars ACM, Golaz J-C, Jacobson AR, Medeiros B. 2012. Climatology of the planetary boundary layer over the continental United States and Europe. *Journal of Geophysical Research*, DOI: 10.1029/2012JD018143.

Seneviratne SI, Corti T, Davin EL, Hirschi M, Jaeger EB, Lehner I, Orlowsky B, Teuling AJ. 2010. Investigating soil moisture-climate interactions in a changing climate: a review. *Earth Science Reviews* **99**: 125–161, DOI: 10.1016/j.earscirev.2010.02.004.

IPCC. 2007. Climate change 2007. In *The Physical Science Basis. Contribution of Working Group I to the Fourth Assessment Report of the Intergovernmental Panel on Climate Change*, Solomon S, Qin D, Manning M, Chen Z, Marquis M, Averyt KB, Tignor M, Miller HL (eds). Cambridge University Press: Cambridge, United Kingdom/New York, NY, USA.

Svensson G, Holtslag AAM, Kumar V, Mauritsen T, Steeneveld GJ, Angevine WM, Bazile E, Beljaars A, de Bruijn EIF, Cheng A, Conangla L, Cuxart J, Ek M, Falk MJ, Freedman F, Kitagawa H, Larson VE, Lock A, Mailhot J, Masson V, Park S, Pleim J, Soderberg S, Weng W, Zampieri M. 2011. Evaluation of the diurnal cycle in the atmospheric boundary layer over land as represented by a variety of single-column models: the second GABLS experiment. *Boundary-Layer Meteorology* **140**: 177–206.

Taylor KE, Stouffer RJ, Meehl GA. 2009. An overview of CMIP5 and the experiment design. *Bulletin of the American Meteorological Society* **93**: 485–498.

Voldoire A, Sanchez-Gomez E, Salas Y Melia D, Decharme B, Cassou C, Senesi S, Valcke S, Beau I, Alias A, Chevallier M, Deque M, Deshayes J, Douville H, Ferneandez E, Madec G, Maisonnave E, Moine M-P, Planton S, Saint-Martin D, Szopa S, Tyteca S, Alkama R, Belamari S, Braun A, Coquart L, Chauvin F. 2012. The CNRM-CM5.1 global climate model: description and basic evaluation. *Climate Dynamics*, DOI: 10.1007/s00382-011-1259-y.

Volodin EM, Dianskii NA, Gusev AV. 2010. Simulating present-day climate with the INMCM4.0 coupled model of the atmospheric and oceanic general circulations. *Izvestiya Atmospheric and Oceanic physics* **46**(4): 448–466.

Vose RS, Easterling DR, Gleason B. 2005. Maximum and minimum temperature trends for the globe: an update through 2004. *Geophysical Research Letters* **32**: L23822.

Wang D, Wang C, Yang X, Lu J. 2005. Winter Northern Hemisphere surface air temperature variability associated with the Arctic Oscillation and North Atlantic Oscillation. *Geophysical Research Letters* **32**: L16706, DOI: 10.1029/2005GL022952.

Watanabe M, Suzuki T, O'ishi R, Komuro Y, Watanabe S, Emori S, Takemura T, Chikira M, Ogura T, Sekiguchi M, Takata K, Yamazaki D, Yokohata T, Nozawa T, Hasumi H, Tatebe H, Kimoto M. 2010. Improved climate simulation by MIROC5: mean states, variability and climate sensitivity. *Journal of Climate* **23**: 6312–6335, DOI: 10.1175/2010JCLI3679.1.

Watanabe S, Hajima T, Sudo K, Nagashima T, Takemura T, Okajima H, Nozawa T, Kawase H, Abe M, Yokohata T, Ise T, Sato H, Kato E, Takata K, Emori S, Kawamiya M. 2011. MIROC-ESM: model description and basic results of CMIP5-20c3m experiments. *Geoscientific Model Development* **4**: 845–872, DOI: 10.5194/gmd-4-845-2011.

Weber RO, Talkner P, Stefanicki G. 1994. Asymmetric diurnal temperature change in the Alpine region. *Geophysical Research Letters* **21**: 673–676.

Zilitinkevich S, Esau I, Baklanov A. 2007. Further comments on the equilibrium height of neutral and stably stratified atmospheric boundary layers. *Quarterly Journal of the Royal Meteorological Society* **133**: 265–271.

Zilitinkevich SS, Elperin T, Kleeorin N, Rogachevskii I, Esau I, Mauritsen T, Miles MW. 2008. Turbulence energetics in stably stratified geophysical flows: strong and weak mixing regimes. *Quarterly Journal of the Royal Meteorological Society* **134**: 793–799, DOI: 10.1002/qj.264.

